



Poly (vinylidene fluoride-co-hexafluoropropylene)/polybenzimidazole blend nanofiber supported Nafion membranes for direct methanol fuel cells

Shih-Hua Wang^a, Hsiu-Li Lin^{a,b,*}

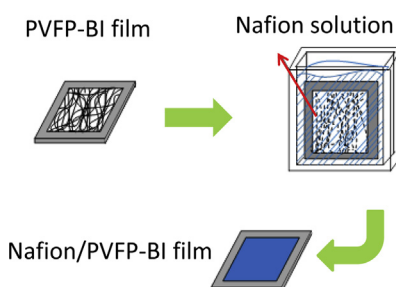
^a Department of Chemical Engineering & Materials Science, Yuan Ze University, Chung-Li, Taoyuan 32003, Taiwan

^b Fuel Cell Center, Yuan Ze University, Chung-Li, Taoyuan 32003, Taiwan

HIGHLIGHTS

- Preparation of PVdF-co-HFP and PBI blend electrospun nanofiber (PVFP-BI) films.
- Preparation of Nafion/PVFP-BI composite membranes by impregnating Nafion into PVFP-BI films.
- Better DMFC performance of Nafion/PVFP-BI than Nafion when blending 5–10 wt.% of PBI in PVFP-BI.

GRAPHICAL ABSTRACT



ARTICLE INFO

Article history:

Received 8 October 2013

Received in revised form

13 January 2014

Accepted 23 January 2014

Available online 2 February 2014

Keywords:

Nafion

Poly (vinylidene fluoride-co-hexafluoropropylene)

Polybenzimidazole

Electrospinning

Direct methanol fuel cell

ABSTRACT

This article presents preparation of poly (vinylidene fluoride-co-hexafluoropropylene) (PVdF-co-HFP) and polybenzimidazole (PBI) blend electrospun nanofiber (PVFP-BI) films from *N,N'*-dimethyl acetamide (DMAc)/acetone mixture solutions. Using the PVFP-BI nanofiber film (thickness ~ 13 – 15 μm) as a supporting material for impregnating Nafion resin solution, Nafion/PVFP-BI composite membranes (thickness ~ 50 μm) are prepared and direct methanol fuel cell (DMFC) tests are performed. Better DMFC performance of the Nafion/PVFP-BI composite membrane than the commercial Nafion-117 (thickness ~ 175 μm) and Nafion-212 (thickness ~ 50 μm) membranes when blending with 5–10 wt.% of PBI in the PVFP-BI nanofiber support film is demonstrated.

© 2014 Elsevier B.V. All rights reserved.

1. Introduction

It is generally accepted that polyelectrolyte membrane fuel cells (PEMFCs) present a promising alternative to traditional power sources due to their high efficiency and non-polluting nature.

* Corresponding author. Department of Chemical Engineering & Materials Science, Yuan Ze University, Chung-Li, Taoyuan 32003, Taiwan. Tel.: +886 3 4638800x2568; fax: +886 3 4559373.

E-mail address: sherry@saturn.yzu.edu.tw (H.-L. Lin).

Nafion (perfluorosulfonated ionomer, Du Pont Co.) membrane is a successful proton exchange membrane (PEM) used as proton-conducting separator in fuel cell utilizing H_2 as a fuel and O_2 (or air) as an oxidant. However, the application of Nafion, as PEMs in DMFCs using methanol as a fuel, causes the problem of *methanol crossover* across the PEM and lowers DMFC performance [1–7]. The methanol crossover results in depolarization loss at cathode thus causing conversion loss by lost fuel. A thicker Nafion PEM, for example commercial Nafion-117 (thickness ~ 175 μm), is mostly used as proton conducting separator in DMFCs. However, the usage

of thicker membrane increases the proton transport resistance across the membrane leading to a higher ohmic resistance thus reduces DMFC performance. As well the thicker Nafion membrane, being an expensive commercial Nafion resin, increases the material cost of DMFC.

In the past decade, researchers have made efforts to reduce methanol crossover through Nafion PEM by employing several methods which include: hybridizing Nafion with low methanol compatible polymers such as poly (vinyl alcohol) (PVA) [8–16], sulfonated poly (ether ether ketone) (s-PEEK) [17], poly-benzimidazole (PBI) [4,18], poly (aniline) (PANI) [19], poly (tetra-fluoroethylene) (PTFE) [20–22], etc., and blending Nafion with inorganic nano-particles such as silicone oxide [23–26], tetraethoxysilane [21,27,28], diphenyl silicate [29], zirconium phosphate (ZrP) [22,30–32], phosphotungstic acid [29], etc. Mixing inorganic nano-particles or blending low methanol compatible polymers into Nafion PEMs reduces methanol crossover across the membranes [8–13,17–33]. However, mixing low methanol compatible modifiers in the Nafion PEMs can also increase proton transfer resistance of the PEMs. Hence, there is an optimum concentration of the low methanol crossover modifier that can be blended in the modified Nafion PEMs resulting in the highest possible DMFC performance.

Recently, researchers have reported that high mechanical strength with low methanol compatible polymer nanofiber thin films supports Nafion resin composite PEMs that can act as successful low methanol crossover PEMs for DMFC applications. These composite PEMs were prepared by impregnating the polymer nanofiber thin film as a supporting material with Nafion resin solution. Some examples of these composite membranes are: porous PTFE thin film impregnated with Nafion resin (i.e., Nafion/PTFE) [20–22,34–38], poly (vinylidene fluoride) (PVdF) electrospun nanofiber thin film impregnated with Nafion resin (i.e., Nafion/PVdF) [39], crosslinked PVA electrospun nanofiber film impregnated with Nafion resin (i.e., Nafion/PVA) [14–16] composite membranes).

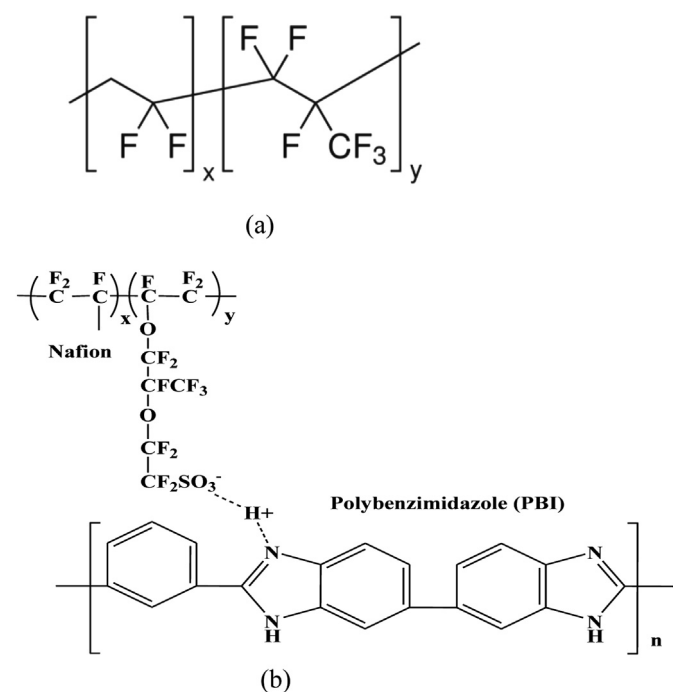


Fig. 1. Chemical structures of polymers. (a) poly (vinylidene fluoride-co-hexafluoropropylene) (PVFP); (b) Interaction of Nafion $-\text{SO}_3\text{H}$ with PBI imidazole group.

Using a high mechanical strength and low methanol compatible fluorocarbon based nanofiber film, for example PTFE [20–22,34–38] and PVdF [39], as supporting materials to impregnate proton conducting Nafion resin allows to reduce the methanol permeability keeping the membrane thickness lower than 50 μm . The lower thickness leads these PEMs to have a lower proton transfer resistance. One of the problem of using the fluorocarbon based nanofiber thin film as a supporting material for impregnating Nafion resin is the poor interface bonding between the Nafion and the fluorocarbon nanofibers, which reduces PEM durability. In order to solve the problem of this poor interface bonding, we, in this study, prepared poly (vinylidene fluoride-co-hexafluoropropylene) (PVFP; Fig. 1a) and polybenzimidazole (PBI) blend (i.e., PVFP-BI) nanofiber films as supporting materials and impregnated it with Nafion resin solution to prepare Nafion/PVFP-BI (i.e., N/PVFP-BI) composite PEMs (thickness $\sim 50 \mu\text{m}$). PBI has been reported as an excellent polymer material for modifying Nafion membrane to reduce methanol crossover [4,18]. The interaction of the imidazole groups of PBI in the PVFP-BI electrospun nanofiber with the sulfonic acid groups of Nafion in the N/PVFP-BI composite PEMs (Fig. 1b) improves the interface bonding between the nanofiber and the Nafion resin. In present work, we demonstrated that blending ~ 5 – $10 \text{ wt.}\%$ of PBI in the PVFP-BI electrospun nanofiber as a supporting material of the N/PVFP-BI composite PEMs could reduce methanol crossover through the membrane and improve DMFC performance.

2. Experimental

2.1. PVFP and PVFP-BI electrospun nanofiber film preparations

2.1.1. Materials

(1-a) PBI was synthesized from 3,3'-diamino benzidine (DABZ, Aldrich Chem. Co.) and isophthalic acid (IPA, Aldrich Chem. Co.) using polyphosphoric acid (PPA, Aldrich Chem. Co.) as solvent. The detailed PBI polymerization procedures were similar to those reported in the literature [40,41]. 5.68 g (0.12 mol) DABZ and 19.92 g (0.12 mol) IPA were mixed with 500 g PPA and polymerized under N_2 atmosphere at 210°C for 48 h. After terminating the polymerization, the product mixture was poured into distilled water to precipitate the PBI product. The precipitated PBI was milled into powder and then mixed with 1 N NaOH solution under stirring for 2 h. During stirring, the NaOH solution was changed at every 30 min to remove residual PPA. The PBI was subsequently rinsed with deionized water several times to remove residual NaOH and then dried under vacuum at 120°C for 24 h. The molecular weight of the as-synthesized PBI was $M_w \sim 1.47 \times 10^5 \text{ g mol}^{-1}$ as determined by gel permeation chromatography (GPC, Jasco PU-2080 plus) using polystyrene as standard. The low molecular weight PBI ($M_w = \sim 1.10 \times 10^4 \text{ g mol}^{-1}$, determined using GPC with polystyrene standard calibration) was obtained from the as-synthesized PBI by fractionating using an *N*-methyl pyrrolidinone (NMP; Aldrich Chemical Co.) and *N*-methylformamide (NMF; Aldrich Chemical Co.) mixture solvent with a NMP/NMF wt. ratio of 3/7 g g^{-1} (in which NMP good and NMF is poor solvent for PBI); (1-b) PVdF-co-HFP (PVFP; $M_w = 455,000$) was purchased from Aldrich Chemical Co., Inc.; (1-c) 5 wt.% Nafion solution (1100 EW, the solvent was a mixture of water, methanol, isopropanol, and unspecified mixed ether) was purchased from Du Pont Co.

2.1.2. Electrospinning process

The electrospinning setup was consisted of a 20 mL syringe with a stainless steel needle (inner diameter = 0.8 mm) connected to its outlet and a collection roll. The syringe with the needle was positioned vertically on a clamp. The collection roll, which was made from copper and covered with aluminum foil, was positioned at a

Table 1

The thickness and compositions of the PVFP and PVFP-BI electrospun nanofiber films.

Nanofiber film	Film thickness L (μm)	PVFP (wt%)	PBI (wt.%)
PVFP	13.4 ± 0.2	100	0
PVFP-BI-9.5-0.5	15.2 ± 0.2	95	5
PVFP-BI-9-1	13.3 ± 0.4	90	10
PVFP-BI-8.5-1.5	14.1 ± 0.3	85	15

distance of 18 cm from the tip of the needle. The PVFP and PBI ($M_w = \sim 1.10 \times 10^4 \text{ g mol}^{-1}$) blend solution used for electrospinning was a 20 wt.% polymer blend in N,N' -dimethyl acetamide (DMAc) and acetone mixture solutions. The solution feeding rate was 1.2 mL h^{-1} and the applied voltage was 18 kV. The nanofiber samples were collected on the aluminum foil. Subsequently, the aluminum foil was removed from the collection roll, and the film sample was kept at ambient environment for at least 24 h before carrying out the characterization. Four electrospun PVFP-BI nanofiber films with thicknesses of ~ 13 – $15 \mu\text{m}$ and PVFP/PBI wt. ratios of 1.0/0.0, 9.5/0.5, 9.0/1.0, 8.5/0.5 were prepared. The thicknesses and compositions of the nanofiber films are summarized in Table 1.

2.2. Impregnation of PVFP and PVFP-BI nanofiber films with Nafion solutions to obtain composite membranes

The PVFP and PVFP-BI nanofiber thin films with thickness of ~ 13 – $15 \mu\text{m}$ as described in Section 2.1 were used to prepare N/PVFP and N/PVFP-BI composite PEMs. The electrospun nanofiber film was mounted on a steel frame and then impregnated in 3.0 wt.% Nafion solution prepared by diluting an as-received 5 wt.% Nafion solution (EW 1100 diluted in a mixture solvent containing water, propanol, methanol, and unspecified ether, Du Pont Co, Inc.) with isopropanol (IPA, Riedel de Haen Co, Ltd), for 4 h and then annealed at 125°C for 20 min. The membrane was then impregnated in 4.0 wt.% Nafion solution (a solution prepared by diluting an as received 5.0 wt.% Nafion solution with isopropanol) for 4 h and then annealed at 125°C for 20 min. Then the membrane was subsequently impregnated in an as received 5.0 wt.% Nafion solution for 4 h and then annealed at 125°C for 20 min. The last process of impregnating nanofiber film in 5 wt.% Nafion solution was repeated several times till the required [Nafion]/[PVFP-BI] (or [Nafion]/[PVFP]) wt. ratio was obtained. Then finally the membranes were further annealed at 125°C for another 90 min. The composition and thickness of N/PVFP and N/PVFP-BI membranes are listed in Table 2.

2.3. Preparation of a Nafion casting membrane

A 5 wt.% Nafion solution was prepared by mixing 33.41 g IPA with 1.67 g Nafion solid which obtained from as-received 5.0 wt.% Nafion solution. The solution was cast in a Petri dish at 60°C for 24 h to evaporate the solvent, and subsequently the membrane was kept at 60°C under vacuum for 6 h to remove the residual solvent. The membranes were then annealed under vacuum at 125°C for

Table 2

The thickness and compositions of N/PVFP and N/PVFP-BI composite membranes.

Membrane	Thickness L (μm)	Fiber film (wt.%)	Nafion (wt.%)
Nafion-117	175.3 ± 0.4	0	100
Nafion-212	50.4 ± 0.6	0	100
Nafion-cast	51.7 ± 0.2	0	100
N/PVFP	53.1 ± 0.2	10	90
N/PVFP-BI-9.5-0.5	48.7 ± 0.3	10	90
N/PVFP-BI-9-1	49.9 ± 0.4	10	90
N/PVFP-BI-8.5-1.5	51.4 ± 0.5	10	90

2 h. The thicknesses of the Nafion casting membrane (i.e., Nafion-cast) is also listed in Table 2.

2.4. Characterizations of N/PVFP, N/PVFP-BI and Nafion cast membranes

2.4.1. Scanning electron microscopy (SEM) and energy dispersion X-ray (EDS) analyses

SEM and EDS (both JSM-5600, Jeol Co., Japan) were used to investigate the morphology of the plane surfaces and cross sections of the N/PVFP and N/PVFP-BI membranes. The samples were coated under vacuum with gold powder before performing the SEM observations.

2.4.2. Conductivity measurements

A device capable of holding the membrane for resistance R measurement was located between the two probes. Before measurement, each membranes was boiled in 0.5 N sulfuric acid solution at 85°C for 1 h and then rinsed with distilled water to clean the residual sulfuric acid ($96.0 \pm 1.0 \text{ wt.}\%$, Fluka Chem. Co., Inc) on the surface of the membranes. The testing device with a membrane was kept in a thermostat under a relative humidity of 95% and the measurements were carried out at 70°C . The ionic conductivity σ was calculated from the measured R value using Eq. (1):

$$\sigma = L/(A \times R) \quad (1)$$

where A (3.14 cm^2) is the cross section area of the membrane for R measurement and L thickness of the membrane. R was measured using an ac impedance system (model SA1125B, Solartron Co., UK). The normalized proton transfer resistance r per unit area of the membrane was obtained from Eq. (2):

$$r = L/\sigma = AR \quad (2)$$

2.4.3. Methanol permeability measurements

Methanol permeability of membranes was measured using an apparatus designed in our lab. The N/PVFP, N/PVFP-BI, and Nafion-cast membranes, stored at 25°C in distilled water for 1 day, were used for methanol permeability P measurements. A device of holding the membranes was located in the middle of two vessels (-a and -b), each of them had a volume of 400 mL. At beginning of methanol permeability test, the source vessel-a was filled with 2 M (6.41 wt.%) methanol (Merck Co., Inc.) aqueous solution and the receiving vessel-b was filled with pure distilled water. The methanol aqueous solution was fed into vessel-a for the measurements. The whole apparatus was kept at 70°C . After methanol crossover through the membrane for a measuring time period t , 2 mL of liquid was taken from vessel-b and its density was measured using a density meter (DA-505, KEM, Japan). The concentration of methanol ($C_b(t)$) of the receiving vessel-b at a measuring time t , was calculated using a standard methanol concentration calibration curve. The standard methanol concentration calibration curve was prepared by plotting measured liquid density data vs. methanol concentrations of the standard methanol aqueous solutions with known concentrations. In the methanol crossover experiment, the methanol concentration $C_b(t)$ of the receiving vessel-b was measured at a time interval of 3600 s. The methanol permeability P of the membrane was obtained from the slope of the plot of $C_b(t)$ vs. t using Eq. (3) [40]:

$$C_b(t) = t \times C_a \times [(P \times A)/(L \times V_b)] \quad (3)$$

where C_a is the wt% of methanol concentration of the aqueous solution in source vessel-a, t (in unit of sec) is the time of each

methanol crossover measurement, A is the cross-section area of the membrane for a methanol crossover measurement, L is the thickness of the membrane, and V_b is the volume of receiving vessel-b. The methanol permeation rate p per unit area of a membrane was obtained from Eq. (4):

$$p = P/L \quad (4)$$

2.5. Direct methanol fuel cell performance test

2.5.1. Membrane electrode assembly (MEA) preparations

The commercial Nafion-117 (EW 1100, thickness $\sim 175 \mu\text{m}$) and Nafion-212 (EW 1100, thickness $\sim 50 \mu\text{m}$) membranes purchased from Du Pont Co. and the Nafion-cast, N/PVFP, N/PVFP-BI membranes prepared in this work were used to prepare MEAs. The gas diffusion layer was a carbon paper (SGL-35BC, SGL Co.). The Pt–Ru catalyst (Johnson Matthey Pt–Ru/C catalyst, 40 wt.% Pt–Ru) loading of the anode was 2.0 mg cm^{-2} and the Pt catalyst (Johnson Matthey Pt/C catalyst, with 40 wt.% Pt) loading of cathode was 1.0 mg cm^{-2} .

2.5.2. DMFC single cell tests

The DMFC single cell performances were tested at 70°C , 80°C , and 90°C using a Globe Tech Computer Cell GT testing system

(Electrochem. Inc.). The anode input methanol aqueous solution flow rate was 5 mL min^{-1} with a methanol feed concentration of 2 M, and the cathode input O_2 flow rate was 150 mL min^{-1} without back pressure. The cell active area was $5 \times 5 \text{ cm}^2$. Before recording the i – V curve, the cell was activated at 0.2 V for 8 h then at 0.3 V for another 8 h to enhance the humidification and activation of MEA.

3. Results and discussion

3.1. Morphologies of PVFP and PVFP-BI electrospun nanofiber films

Fig. 2a–c illustrates the SEM micrographs with fiber diameter distributions of PVFP nanofiber film electrospun from 20 wt.% PVFP in three DMAc/acetone mixture solvents, i.e., [DMAc]/[acetone] = 10/0, 9/1, and 8/2 g g^{-1} , respectively. These micrographs demonstrate presence of beads in the electrospun nanofibers at less than 10 wt.% acetone content in the acetone/DMAc mixture solvents of the PVFP electrospinning solutions (Fig. 2a and b). When the acetone content of the acetone/DMAc mixture solvents of the PVFP electrospinning solutions was increased to 20 wt.%, smooth electrospun nanofibers without beads were obtained as shown in

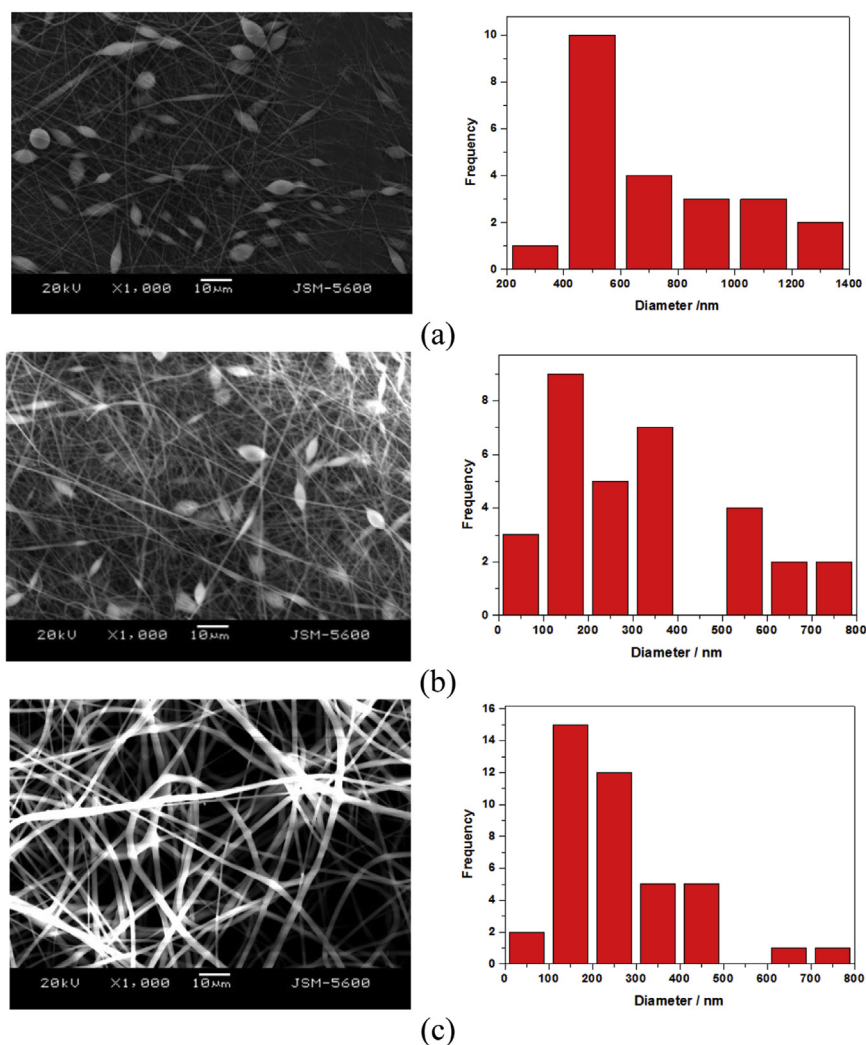


Fig. 2. SEM micrographs ($\times 1000$) (left column) and diameter distribution (right column) of poly (vinylidene fluoride-co-hexafluoropropylene) (PVFP) nanofiber films electrospun from 20 wt.% PVFP in DMAc and acetone mixture solvents. The wt. ratios of DMAc/acetone are: (a) DMAc/acetone = 10/0 g g^{-1} ; (b) DMAc/acetone = 9/1 g g^{-1} ; (c) DMAc/acetone = 8/2 g g^{-1} .

Fig. 2c. Thus the mixture solvent with a [DMAC]/[acetone] wt. ratio of 8/2 was used to prepare PVFP/PBI blend solutions and to perform electrospinning in the following sections.

Fig. 3a–c shows the SEM micrographs and fiber diameter distributions of PVFP-BI nanofiber films electrospun from PVFP/PBI blend in DMAc/acetone ([DMAC]/[acetone] = 8/2 g g⁻¹) mixture solutions with [PVFP]/[PBI] wt. ratios of 9.5/0.5 g g⁻¹, 9.0/1.0 g g⁻¹, and 8.5/1.5 g g⁻¹, respectively. These micrographs demonstrate smooth fiber surface with no bead observed in the PVFP-BI blend electrospun nanofibers. The PVFP-BI electrospun fiber films were not obtained when PBI concentration of the PVFP/PBI blend was higher than 15 wt.%. As the PBI concentration of the PVFP/PBI blend was above 15 wt.%, the polymer blend was not well dissolved in the DMAc/acetone mixture solution due to the poor compatibility of PBI with the solvent acetone.

3.2. FTIR analyses of PVFP electrospun and PVFP-BI electrospun nanofiber films

Fig. 4 illustrates the IR spectra of PBI (spectrum-e) and PVFP (spectrum-a), PVFP-BI-9.5-0.5 (spectrum-b), PVFP-BI-9-1 (spectrum-c), PVFP-BI-8.5-1.5 (spectrum-d) electrospun nanofiber films. In Fig. 4, the three vertical lines indicate the PBI imidazole C–N

stretch (~ 1300 cm⁻¹), ring in-plane =C–H bending vibration (1000 cm⁻¹), and ring out-of-plane =C–H bending vibration (800 cm⁻¹). These three imidazole absorption peak intensities shows increase in Fig. 4d compare to Fig. 4a, indicating the increasing PBI content in the PVFP-BI blend electrospun fiber according to the sequence of PVFP < PVFP-BI-9.5-0.5 < PVFP-BI-9-1 < PVFP-BI-8.5-1.5, which was consistent with original fed [PVFP]/[PBI] wt. ratios for preparing electrospun nanofiber films.

3.3. SEM morphology studies of N/PVFP and N/PVFP-BI composite membranes

The morphologies of the composite membranes of electrospun nanofiber films impregnated with Nafion resin were also investigated using SEM. Fig. 5a–d shows the SEM micrographs of the plane surfaces of the N/PVFP, N/PVFP-BI-9.5-0.5, N/PVFP-BI-9-1, and N/PVFP-BI-8.5-1.5 composite membranes, respectively. Fig. 6a–d demonstrates the SEM micrographs of the cross sections of the N/PVFP, N/PVFP-BI-9.5-0.5, N/PVFP-BI-9-1, and N/PVFP-BI-8.5-1.5 composite membranes, respectively. These micrographs revealed smooth plane surfaces without any visible void inside the membranes, indicating good impregnation of Nafion resin into the nanofiber films.

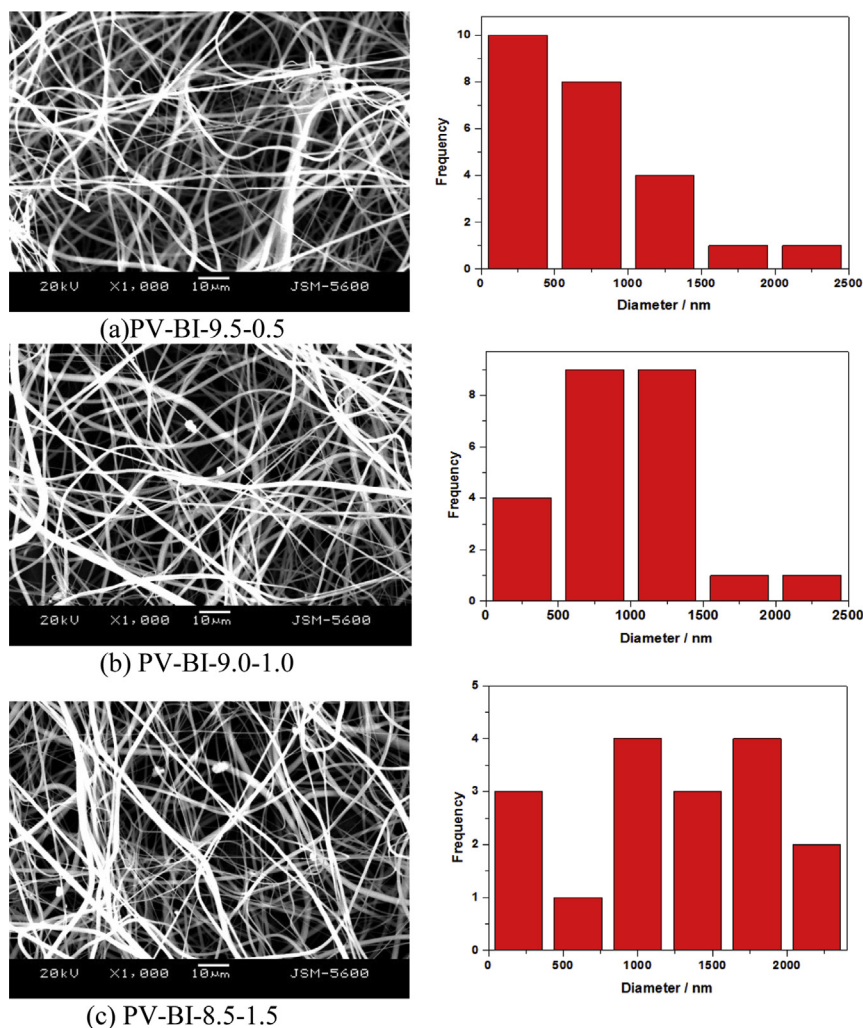


Fig. 3. SEM micrographs ($\times 1000$) of nanofiber films electrospun from PVFP–PBI blend in DMAc/acetone (8/2 by wt.) mixture solutions. The wt. ratios of [PVFP]/[PBI] are: (a) [PVFP]/[PBI] = 9.5/0.5 g g⁻¹; (b) [PVFP]/[PBI] = 9.0/1.0 g g⁻¹; (c) [PVFP]/[PBI] = 8.5/1.5 g g⁻¹.

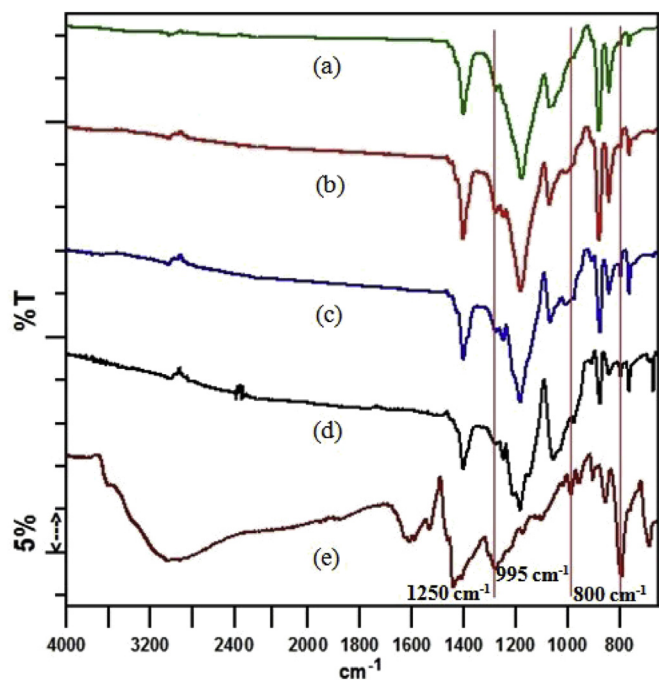


Fig. 4. FTIR spectra of poly (vinylidene fluoride-co-hexafluoropropylene) (PVFP) and poly (benzimidazole) (PBI) and electrospun nanofibers of PVFP/PBI (PVFP-BI) blends. From top to bottom: (a) PVFP; (b) PVFP-BI-9.5-0.5; (c) PVFP-BI-9-1; (d) PVFP-BI-8.5-1.5; (e) PBI. The three vertical lines indicate the PBI functional groups C–N stretch ($\sim 1250\text{ cm}^{-1}$), ring in-plane =C–H bending vibration (995 cm^{-1}), and ring out-of-plane =C–H bending vibration (800 cm^{-1}).

3.4. Conductivities of N/PVFP and N/PVFP-BI composite membranes

The resistances R of the Nafion-117, Nafion-212, Nafion-cast, N/PVFP, N/PVFP-BI-9.5-0.5, N/PVFP-BI-9-1, and N/PVFP-BI-8.5-1.5 composite membranes were measured, and σ and r (i.e., $r = L/\sigma$) data of these membranes were calculated from R using Eqs. (1) and (2), respectively. The R , σ , and r values of all these PEMs are summarized in Table 3. Table 3 shows that the σ of the Nafion-117, Nafion-212, and Nafion-cast membranes was larger than those of the N/PVFP, N/PVFP-BI-9.5-0.5, N/PVFP-BI-9-1, and N/PVFP-BI-8.5-1.5 membranes. The proton conductivities of both PVFP and PBI were worse than that of Nafion. Introducing PVFP and PVFP-BI nanofiber films in the Nafion membrane caused reduction in the membrane conductivity. These data also revealed that σ of the composite membranes decreased with increasing the PBI content of the PVFP-BI nanofibers. It could be possible that the interaction of PBI imidazole C=N– with the Nafion $-\text{SO}_3\text{H}$ resulted in a decrease in the free $-\text{SO}_3\text{H}$ groups, leading to a decrease of σ of the composite membrane when the PBI content of the PVFP-BI nanofibers was increased. It is the combination of σ and L (i.e., $r = L/\sigma$) rather than σ alone that determines the resistance of the proton transfer per unit area in a membrane and thus the DMFC performance of the membrane. These data demonstrated that the L/σ value of Nafion-117 was larger than those of the Nafion-212, Nafion-cast, and N/PVFP and N/PVFP-BI composite membranes because of higher thickness of Nafion-117 membrane. Table 3 also demonstrated that the L/σ value increased according to the sequence: Nafion-212 < Nafion-cast < N/PVFP < N/PVFP-BI-9.5-0.5 < N/PVFP-BI-9-1 < N/PVFP-BI-8.5-1.5. The Nafion-212, Nafion-cast, and N/PVFP and N/PVFP-BI composite membranes had similar membrane thickness, the larger L/σ value of a membrane can be attributed to its lower σ value.

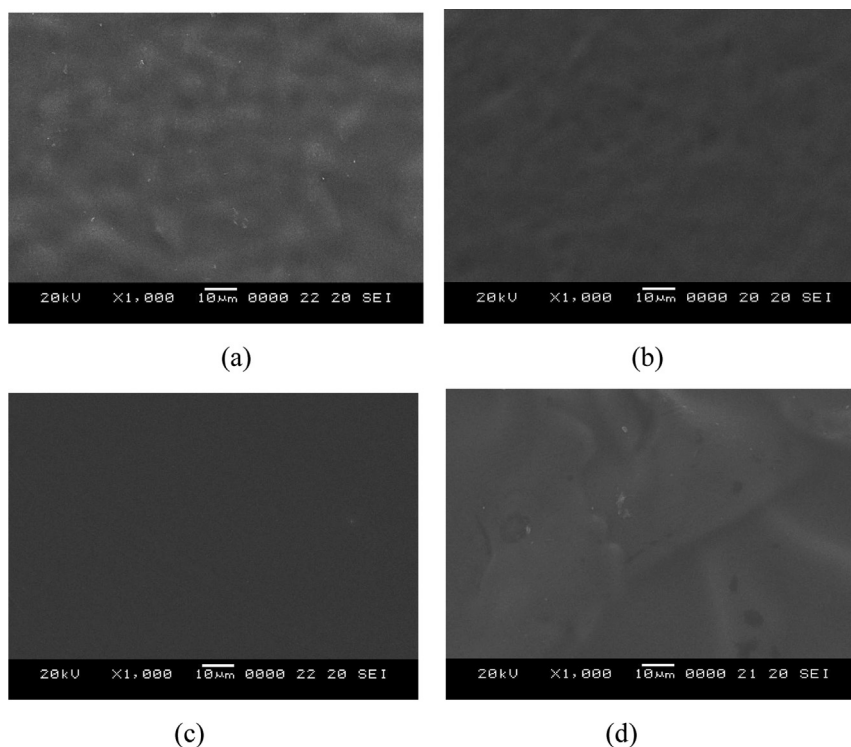


Fig. 5. SEM micrographs ($\times 1000$; scale bar $10\text{ }\mu\text{m}$) of the plane surfaces of the N/PVFP-BI composite membranes. (a) N/PVFP; (b) N/PVFP-BI-9.5-0.5; (c) N/PVFP-BI-9-1; (d) N/PVFP-BI-8.5-1.5.

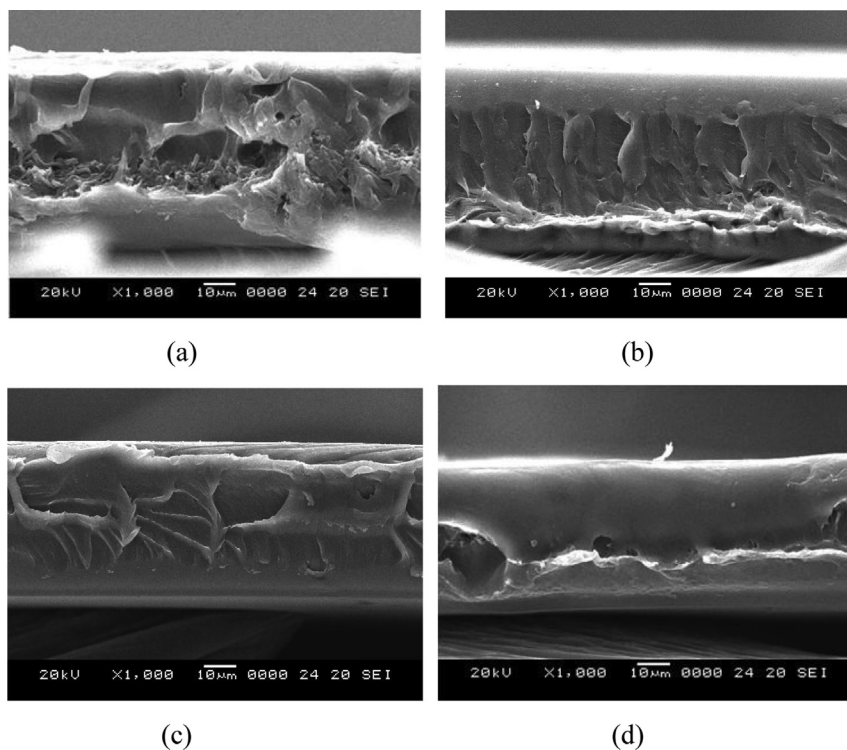


Fig. 6. SEM micrographs ($\times 1000$; scale bar $10\ \mu\text{m}$) of the cross sections of the N/PVFP-BI composite membranes. (a) N/PVFP; (b) N/PVFP-BI-9.5-0.5; (c) N/PVFP-BI-9-1; (d) N/PVFP-BI-8.5-1.5.

3.5. Methanol permeability of membranes

Methanol permeability measurements of the Nafion-117, Nafion-212, Nafion-cast, and N/PVFP and N/PVFP-BI composite membranes were carried out at $70\ ^\circ\text{C}$ with a methanol fed concentration $C_a = 2\ \text{M}$ (6.41 wt.%). Fig. 7a and b illustrates the plots of Eq. (3), i.e., $C_b(t)$ vs. t , of the methanol permeability measurements for all the membranes and the N/PVFP and N/PVFP-BI composite membranes. The methanol permeability P of each membrane was calculated from the slope of the $C_b(t)$ vs. t plot. Table 4 summarizes the P and $p = P/L$ (the methanol permeation rate per unit area of a membrane) data for the membranes. The P value decreased in the sequence of Nafion-cast > Nafion-212 > Nafion-117 > N/PVFP > N/PVFP-BI-9.5-0.5 > N/PVFP-BI-9-1 > N/PVFP-BI-8.5-1.5, and the P/L value decreased in the sequence of Nafion-cast > Nafion-212 > Nafion-117 > N/PVFP > N/PVFP-BI-9.5-0.5 > N/PVFP-BI-9-1 > N/PVFP-BI-8.5-1.5. All of the N/PVFP and N/PVFP-BI membranes had lower P and P/L values than the Nafion-117, Nafion-212, and Nafion-cast

membranes. These results suggested that both PVFP and PBI possess lower methanol affinity than Nafion; and the PVFP and PVFP-BI nanofiber films are good modifiers to reduce the methanol crossover through the Nafion membrane.

Among the three neat Nafion membranes, Nafion-117 had a smaller P/L value than the Nafion-212 and Nafion-cast, due to the higher thickness of the Nafion-117 ($\sim 175\ \mu\text{m}$) than the Nafion-212 ($\sim 50\ \mu\text{m}$) and Nafion-cast ($\sim 52\ \mu\text{m}$). Owing to the similar membrane thickness ($\sim 50\ \mu\text{m}$), the smaller P/L values of the N/PVFP and N/PVFP-BI membranes than the Nafion-212 and Nafion-cast membranes can be attributed to the presence of lower methanol affinity of PVFP and PVFP-BI nanofibers in the composite membranes. Table 4 and Fig. 7 also demonstrate that both the P and P/L values of the N/PVFP and N/PVFP-BI composite membranes decreased with increasing the PBI content of the PVFP-BI nanofibers. The interaction of the PBI imidazole $-\text{C}=\text{N}-$ groups with the Nafion $-\text{SO}_3\text{H}$ groups reduced the free $-\text{SO}_3\text{H}$ groups, which possess higher affinity for methanol and water than PBI and PVFP, and thus reduced P and P/L values of the N/PVFP-BI membranes.

A careful investigation of the data shown in Tables 3 and 4 revealed that L/σ increased and P/L decreased for Nafion-cast, N/PVFP, and N/PVFP-BI membranes. These results suggested that the methanol crossover through the membrane decreased and the proton conducting resistance increased with the presence of PVFP and the increase of the PBI content in the PVFP-BI nanofiber of the membranes. The decrease of the methanol crossover through the membrane increases the OCV of DMFC and improves the DMFC performance. However, the increase in the proton conducting resistance results in an increase in the ohmic loss of the membrane thus decreases the DMFC performance. There is an optimum condition in the N/VA-f membranes for the highest DMFC performance as being discussed in the next section.

Table 3

Composition, thickness L , resistance R , and conductivity σ of membranes (temp = $70\ ^\circ\text{C}$; RH = 95%; $A = 3.14\ \text{cm}^2$).

Membrane	[PVdFHP]/ [PVA] g g ⁻¹	$R\ 10^{-1}\ \Omega$	$\sigma\ 10^{-2}\ \text{S cm}^{-1}$	$r = L/\sigma\ 10^{-1}\ \Omega\ \text{cm}^2$
Nafion-117	—	2.9 ± 0.1	1.9 ± 0.1	9.2 ± 0.5
Nafion-212	—	0.8 ± 0.2	2.0 ± 0.4	2.5 ± 0.5
Nafion-cast	—	0.9 ± 0.1	1.8 ± 0.1	2.9 ± 0.5
N/PVFP	10.0/0	1.1 ± 0.1	1.6 ± 0.1	3.4 ± 0.6
N/PVFP-BI-9.5-0.5	9.5/0.5	1.3 ± 0.2	1.3 ± 0.1	3.9 ± 0.7
N/PVFP-BI-9-1	9.0/1.0	1.5 ± 0.3	1.1 ± 0.1	4.7 ± 0.5
N/PVFP-BI-8.5-1.5	8.5/1.5	1.8 ± 0.4	0.9 ± 0.2	6.0 ± 0.6

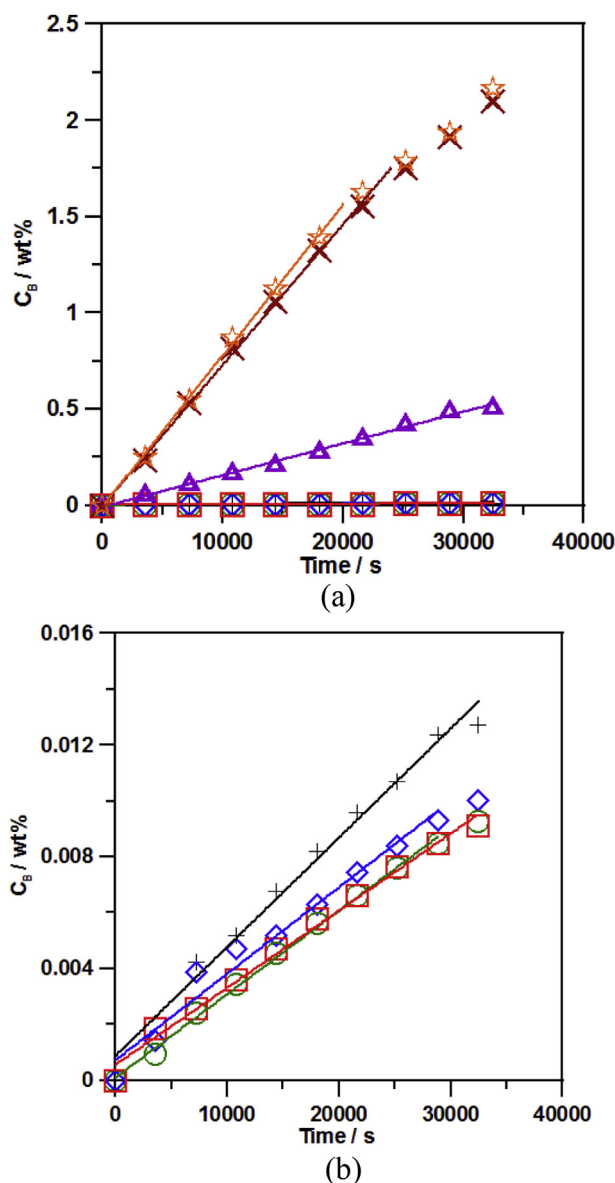


Fig. 7. Plots of $C_b(t)$ vs. t of Eq. (3). Temp = 70 °C, methanol fed concentration $C_a = 2$ M (6.41 wt.%). (a) Plots of all the membranes; (b) Plots of N/PVFP and N/PVFP-BI composite membranes. Membranes: (Δ) Nafion-117; (\times) Nafion-212; ($*$) Nafion-cast; (+) N/PVFP; (\diamond) N/PVFP-BI-9.5-0.5; (\circ) N/PVFP-BI-9-1; (\square) N/PVFP-BI-8.5-1.5.

3.6. DMFC single cell performance studies

The Nafion-117, Nafion-112, Nafion-cast, N/PVFP, and N/PVFP-BI membranes were used to prepare MEAs and to carry out DMFC single cell performance tests. Fig. 8a–c shows the data of single cell potential V vs. current density i for DMFCs operated at 70 °C, 80 °C and 90 °C, respectively. The methanol concentration of the aqueous solution fed in the anode was 2 M. The power density $PD(i) = V(i) \times i$ at a current density i of each MEA can be estimated from the single cell test i – V curve. The maximum power density PD_{\max} of each MEA was estimated from the $PD(i)$ vs. i data. Table 5 summarizes the unit cell test open circuit voltage (OCV) and PD_{\max} data of the MEAs prepared from these membranes.

DMFC test results demonstrated that the OCV of the MEAs decreased with various PEMs according to the sequence: Nafion-

Table 4

Methanol permeability of membranes. Temp = 70 °C.

Membrane	P (10^{-8} cm ² s ⁻¹)	$p = P/L$ (10^{-6} cm s ⁻¹)	σ/P (10^5 S cm ⁻³ s)
$C_a = 2$ M (6.41 wt.%)			
Nafion-117	420 ± 4	240 ± 5	0.045 ± 0.006
Nafion-212	489 ± 6	940 ± 10	0.040 ± 0.008
Nafion-cast	509 ± 7	984 ± 2	0.035 ± 0.007
N/PVFP	2.66 ± 0.03	5.02 ± 0.04	6.0 ± 0.6
N/PVFP-BI-9.5-0.5	1.88 ± 0.02	3.81 ± 0.06	6.9 ± 0.05
N/PVFP-BI-9-1	1.86 ± 0.01	3.79 ± 0.04	5.9 ± 0.4
N/PVFP-BI-8.5-1.5	1.81 ± 0.01	3.51 ± 0.05	5.0 ± 0.5

117 > N/PVFP-BI-8.5-1.5 ~ N/PVFP-BI-9-1 > N/PVFP-BI-9.5-0.5 > N/PVFP ~ Nafion-212 > Nafion-cast. These results were consistent with the P/L data shown in Table 4, which showed that the P/L value increased with the PEMs according to the sequence of Nafion-cast > Nafion-212 > Nafion-117 > N/PVFP > N/PVFP-BI-9.5-0.5 > N/PVFP-BI-9-1 > N/PVFP-BI-8.5-1.5. The PD_{\max} of these MEAs decreased with PEMs according to the sequence: N/PVFP-BI-9.5-0.5 > N/PVFP-BI-9-1 > N/PVFP ~ N/PVFP-BI-8.5-1.5 > Nafion-117 > Nafion-212 > Nafion-cast. We can find the blending 0–15 wt.% of PBI in the PVFP-BI nanofiber film as a support of Nafion resin reduced the conductivity and the methanol crossover through the PEM. The effect of conductivity decrease and the methanol crossover increase on DMFC performance are just the opposite. Table 4 shows the ratio between conductivity and methanol permeability for these membranes. The ratio between conductivity and methanol permeability decreased with various membranes according to the sequence: N/PVFP-BI-9.5-0.5 > N/PVFP ~ N/PVFP-BI-9-1 > N/PVFP-BI-8.5-1.5 > Nafion-117 > Nafion-212 > Nafion-cast. The result is consistent with the PD_{\max} data. These results suggested that blending 5–10 wt.% of PBI in the PVFP-BI nanofiber film as a support of Nafion resin enhance the DMFC performance, arising from reducing the methanol crossover through the PEM, and compensated for the reduced conductivity. However, increasing the PBI content of PVFP-BI nanofiber above 15 wt.% caused high interaction of Nafion –SO₃H with PBI imidazole, leading to an increase in the proton transfer resistance through the PEM and a reduction of DMFC performance.

4. Conclusions

It is known that the commercial Nafion-117 (thickness ~175 μm) membrane has a better DMFC performance than the Nafion-212 (thickness ~50 μm) membrane, due to the higher membrane thickness of Nafion-117, which causes lower methanol crossover through the membrane. In this work, we demonstrated that use of PVFP-BI nanofiber film as a Nafion resin membrane support can reduce methanol crossover through the membrane, which allowed reduction in the membrane thickness lower than Nafion-117 resulting in a better DMFC performance than Nafion-117. Though the presence of PVFP-BI nanofiber film in the Nafion membrane also caused a decrease in the proton conductivity σ of the membrane, however, the lower membrane thickness compensated for the reduced conductivity. The interaction of the imidazole –C=N– group of the PVFP-BI nanofiber with the –SO₃H group of Nafion resulted in decreasing both the proton conductivity (which led to a lower DMFC performance) and the methanol crossover (which led to higher DMFC performance) of the membrane. We showed that 5–10 wt.% PBI in the PVFP-BI nanofiber film as a Nafion resin membrane support is an optimum PBI content of a N/PVFP-BI membrane for the highest DMFC performance.

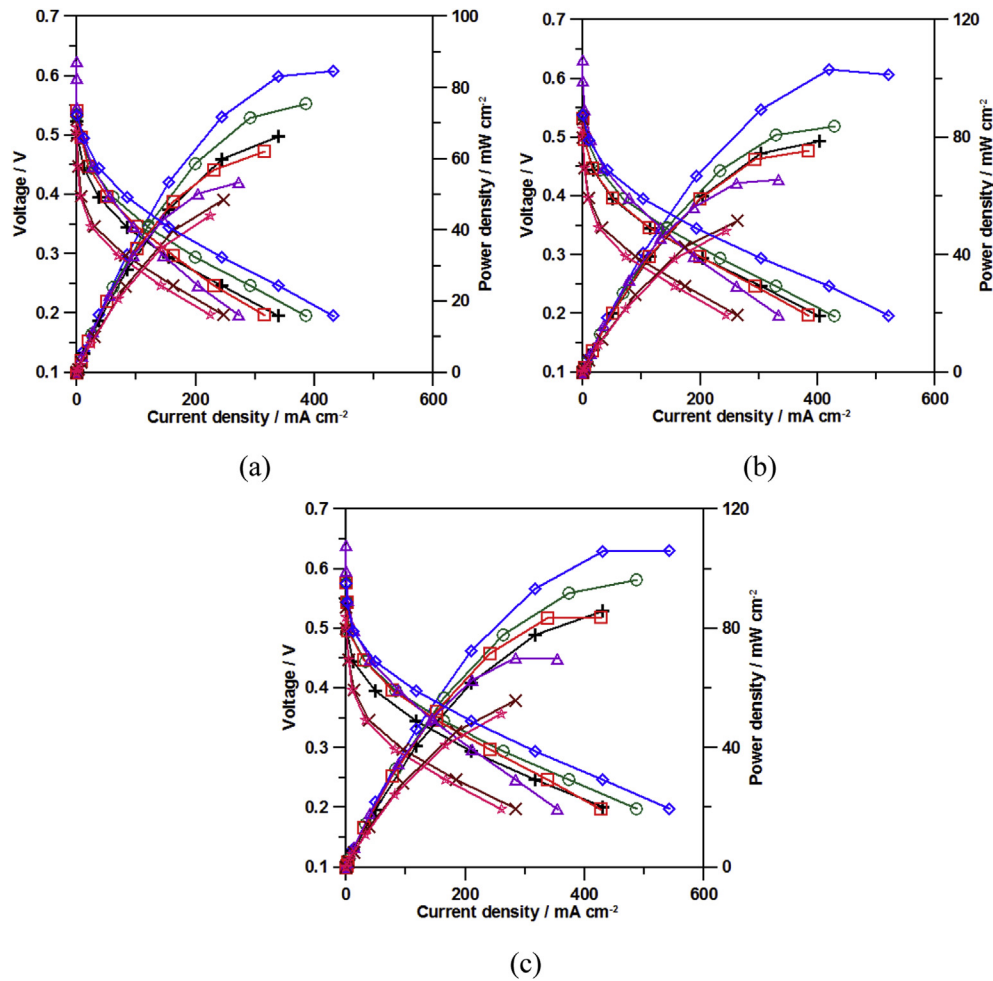


Fig. 8. DMFC *i*–*V* and *i*–*PD* curves of MEAs prepared from Nafion/PVFP–PBI nanofiber composite membranes, Nafion-117, and Nafion-212 membranes at (a) 70 °C; (b) 80 °C; (c) 90 °C. (Δ) Nafion-117; (×) Nafion-212; (*) Nafion-cast; (+) N/PVFP; (◇) N/PVFP-BI-9.5-0.5; (○) N/PVFP-BI-9-1; (□) N/PVFP-BI-8.5-1.5.

Table 5
Unit cell test OCV and *PD*_{max} data. Temp 70 °C, 80 °C, and 90 °C. Anode methanol fed concentration 2 M.

Membrane	OCV (V)	<i>PD</i> _{max} (mW cm ^{−2})
Temp 70 °C		
Nafion-117	0.625	53.6
Nafion-212	0.527	48.6
Nafion-cast	0.513	44.0
N/PVFP	0.524	66.4
N/PVFP-BI-9.5-0.5	0.529	84.6
N/PVFP-BI-9-1	0.535	75.5
N/PVFP-BI-8.5-1.5	0.541	62.2
Temp 80 °C		
Nafion-117	0.633	65.7
Nafion-212	0.532	51.8
Nafion-cast	0.518	48.1
N/PVFP	0.531	78.9
N/PVFP-BI-9.5-0.5	0.541	103.0
N/PVFP-BI-9-1	0.545	83.3
N/PVFP-BI-8.5-1.5	0.547	75.4
Temp 90 °C		
Nafion-117	0.639	70.0
Nafion-212	0.540	55.8
Nafion-cast	0.527	51.3
N/PVFP	0.555	86.0
N/PVFP-BI-9.5-0.5	0.571	106.2
N/PVFP-BI-9-1	0.575	96.3
N/PVFP-BI-8.5-1.5	0.577	83.9

Acknowledgments

The authors would like to thank the National Science Council for the financial support through grant no. NSC-101-2221-E-155-027.

References

[1] J. Muller, G. Frank, K. Colbow, D. Wilkinson, in: W. Vielstich, A. Lamm, H.A. Gasteiger (Eds.), Handbook of Fuel Cells- Fundamentals Technology and Applications, vol. 4, John Wiley & Sons Ltd, 2003, pp. 847–855.
[2] G. Cacciola, V. Antonucci, S. Freni, J. Power Sources 100 (2001) 67–79.
[3] M. Neergat, K.A. Friedrich, U. Stimming, in: W. Vielstich, A. Lamm, H.A. Gasteiger (Eds.), Handbook of Fuel Cells – Fundamentals Technology and Applications, vol. 4, John Wiley & Sons Ltd, 2003, pp. 856–877.
[4] K. Scott, W.M. Taama, P. Argyropoulos, K. Sundmacher, J. Power Sources 83 (1999) 204–216.
[5] T. Schultz, S. Zhou, K. Sundmacher, Chem. Eng. Technol. 24 (2001) 1223–1233.
[6] K. Scott, W. Taama, J. Cruickshank, J. Power Sources 65 (1997) 159–171.
[7] G. Murgia, L. Pisani, A.K. Shukla, K. Scott, J. Electrochem. Soc. 150 (9) (2003) A1231–A1245.
[8] B.S. Pivovar, Y. Wang, E.L. Cussler, J. Membr. Sci. 154 (1999) 155–162.
[9] Z.G. Shao, X. Wang, I.M. Hsing, J. Membr. Sci. 210 (2002) 147–153.
[10] Z.G. Shao, I.M. Hsing, Electrochem. Solid State Lett. 5 (2002) A185–A187.
[11] W. Xu, C. Liu, X. Xue, Y. Su, Y. Lv, W. Xing, T. Lu, Solid State Ionics 171 (2004) 121–127.
[12] N.W. DeLuca, Y.A. Elabd, J. Membr. Sci. 282 (2006) 217–224.
[13] N.W. DeLuca, Y.A. Elabd, J. Power Sources 163 (2006) 386–391.
[14] H.L. Lin, S.H. Wang, C.K. Chiu, T.L. Yu, L.C. Chen, C.C. Huang, T.H. Cheng, J.M. Lin, J. Membr. Sci. 365 (2010) 114–122.
[15] S. Molla, V. Compan, J. Membr. Sci. 372 (2011) 191–200.
[16] S. Molla, V. Compan, J. Power Sources 196 (2011) 2699–2708.

- [17] J.C. Tsai, H.P. Cheng, J.F. Kuo, Y.H. Huang, C.Y. Chen, *J. Power Sources* 189 (2009) 958–965.
- [18] A. Ainla, D. Brandell, *Solid State Ionics* 178 (2007) 581–585.
- [19] C.H. Wang, C.C. Chen, H.C. Hsu, H.Y. Du, L.C. Chen, H.C. Shih, J. Stejskal, K.H. Chen, C.P. Chen, J.Y. Huang, *J. Power Sources* 190 (2009) 279–284.
- [20] H.L. Lin, T.L. Yu, L.N. Huang, L.C. Chen, K.S. Shen, G.B. Chung, *J. Power Sources* 150 (2005) 11–19.
- [21] L.N. Huang, L.C. Chen, T.L. Yu, H.L. Lin, *J. Power Sources* 161 (2006) 1096–1105.
- [22] L.C. Chen, T.L. Yu, H.L. Lin, S.H. Yeh, *J. Membr. Sci.* 307 (2008) 10–20.
- [23] K.T. Adjemian, S.J. Lee, S. Srinivasan, J. Benzigerb, A.B. Bocarsly, *J. Electrochem. Soc.* 149 (3) (2002) A256–A261.
- [24] K.T. Adjemian, S. Srinivasan, J. Benzigerb, A.B. Bocarsly, *J. Power Sources* 109 (2002), 356–364.
- [25] D.H. Jung, S.Y. Cho, D.H. Peck, D.H. Peck, D.R. Shin, J.S. Kim, *J. Power Sources* 71 (1/2) (1998) 169–173.
- [26] G.Q. Lu, C.Y. Wang, T.J. Yen, X. Zhang, *Electrochim. Acta* 49 (2004) 821–828.
- [27] K.A. Mauritz, J.T. Payne, *J. Membr. Sci.* 168 (2000) 39–51.
- [28] Q. Deng, R.B. Moore, K.A. Mauritz, *J. Appl. Polym. Sci.* 68 (1998) 747–763.
- [29] Z.X. Linag, T.S. Zhao, J. Prabhuram, *J. Membr. Sci.* 283 (2006) 219–224.
- [30] Y. Si, H.R. Kunz, J.M. Fenton, *J. Electrochem. Soc.* 151 (2004) A623–A631.
- [31] C. Yang, S. Srinivasan, A.S. Arisco, P. Creti, *Electrochem. Solid State Lett.* 4 (2001) A31–A34.
- [32] V.S. Silva, B. Ruffmann, H. Silva, V.B. Silva, A. Mendes, L.M. Maderia, S. Nunes, *J. Membr. Sci.* 284 (2006) 137–144.
- [33] W. Xu, T. Lu, C. Liu, W. Xing, *Electrochim. Acta* 50 (2005) 3280–3285.
- [34] C. Liu, C.R. Martin, *J. Electrochem. Soc.* 137 (1990) 510–517.
- [35] C. Liu, C.R. Martin, *J. Electrochem. Soc.* 137 (1990) 3114–3120.
- [36] B. Bahar, A.R. Hobson, J. Kolde, *US Patent* 5,547,551, 1996.
- [37] K.M. Nouel, P.S. Fedkiw, *Electrochim. Acta* 43 (1998) 2381–2387.
- [38] F. Liu, B. Yi, D. Xing, J. Yu, H. Zhang, *J. Membr. Sci.* 212 (2003) 213–223.
- [39] S.W. Choi, Y.Z. Fu, Y.R. Ahn, S.M. Jo, A. Manthiram, *J. Power Sources* 180 (2008) 167–171.
- [40] Y. Iwakura, K. Uno, Y. Imai, *J. Polym. Sci. A 2* (1964) 2605–2615.
- [41] H.L. Lin, Y.C. Chou, T.L. Yu, S.W. Lai, *Int. J. Hydrogen Energy* 37 (2012) 383–392.